

Probability-Possibility Theories Based Iris Biometric Recognition System

Majd BELLAJ, Imen KHANFIR KALLEL and Dorra SELLAMI

CEM Lab, National Engineering School of Sfax, University of Sfax, 3038 Sfax, Tunisia (iTi) Department, IMT Atlantique, France

Received 17th of June 2017; accepted 30th march 2019

Abstract

The performance and robustness of the iris-based recognition systems still suffer from imperfection in the biometric information. This paper makes an attempt to address these imperfections and deals with important problem for real system. We proposed a new method for iris recognition system based on uncertainty theories to treat imperfection iris feature. Several factors cause different types of degradation in iris data such as the poor quality of the acquired pictures, the partial occlusion of the iris region due to light spots, or lenses, eyeglasses, hair or eyelids, and adverse illumination and/or contrast. All of these factors are open problems in the field of iris recognition and affect the performance of iris segmentation, its feature extraction or decision making process, and appear as imperfections in the extracted iris feature. The aim of our experiments is to model the variability and ambiguity in the iris data with the uncertainty theories. This paper illustrates the importance of the use of this theory for modeling or/and treating encountered imperfections. Several comparative experiments are conducted on two subsets of the CASIA-V4 iris image database namely Interval and Synthetic. Compared to a typical iris recognition system relying on the uncertainty theories, experimental results show that our proposed model improves the iris recognition system in terms of Equal Error Rates (EER), Area Under the receiver operating characteristics Curve (AUC) and Accuracy Recognition Rate (ARR) statistics.

Key Words: Iris Biometric Recognition System, Iris Feature Imperfections, Probability Theory, Possibility Theory.

1 Introduction

Iris recognition system [1] is the process of recognizing a person by analyzing the random pattern of his iris. The iris is the colored part of the eye and is around the pupil of every human being. In fact, it is a muscle within the eye that regulates the size of the pupil, controlling the amount of light that enters the eye. This

Correspondence to: majd.bellaj@gmail.com

Recommended for acceptance by <Dr Angel Sappa>

DOI : <https://doi.org/10.5565/rev/elcvia.1132>

ELCVIA ISSN: 1577-5097

Published by Computer Vision Center / Universitat Autònoma de Barcelona, Barcelona, Spain

biometric trait has a distinct texture containing randomly distributed and irregularly shaped microstructures, unique and informative texture patterns. The current research of the human iris could be classified into three main categories namely: the iris segmentation [2],[3], feature extraction and iris signature [4],[5], eyelid or eyelash detection [6], and compensation of eye rotation and iris texture deformation [7].

The efficiency and robustness of the human iris are greatly relying on the quality of the captured biometric sample. Recently, a great deal of research [3],[8],[9] was applied on non ideal iris images. There are many situations where the iris texture is damaged, e.g. in the case of lenses, eyeglasses, hair, motion blur, non-linear, deformed, ageing or adverse illumination and compression. All of these affect the iris template (the extracted iris feature). Therefore, it is imperative to first analyze the iris data and look for correcting the type of imperfections induced. Such imperfections can be classified into two main groups: imprecision and uncertainty [10]. Depending on the imperfection type, the state-of-the-art offers several tools proposed to deal with uncertain information such as, probability theory, fuzzy set theory [11], evidence theory [12] and possibility theory [13]. Given the diversity of these uncertainty theories, we aim to choose the best method that can be adapted to our context.

The specificity of the iris biometric data suggests a model able to deal with both ambiguity and variability. The probability theory was the first uncertainty theory that handles imperfect information but seems to be inappropriate due to its limitation in managing uncertainty without being able to handle imprecision. Furthermore, the fuzzy set theory is well suited for modeling imprecision and more specifically, ambiguity but it is unable to handle uncertainty. Fortunately, the evidence theory is able to model some types of uncertain or imprecise information. Such formalism is provided by the possibility theory.

The possibility theory seems to fit best our proposed iris recognition system. Indeed, this uncertainty theory is a natural and flexible tool for representing imperfect information that is uncertain, more precisely variability and imprecise, more precisely ambiguity. Zadeh [14] was the first to introduce this theory and, subsequently, it was improved by several other authors, like Dubois and Prade [13], Cooman and Aeyels [15] among others. This theory has developed rapidly in recent years and has been widely used in various fields such as, diagnosis [16], obstacle avoidance systems and electronic travel aids (ETA) [17], and biometrics [18],[19].

In the possibility theory, the possibility distribution [15] is an essential concept, that can be derived from the collected data. This theory is related to other theories [20], such as, the probability theory, the fuzzy set theory and the belief function theory. The transformations (probabilistic-possibilistic, membership function-possibilistic or basic belief assignment-possibilistic) applied to these rules are often accompanied with a loss of information, i.e., an increase of imperfection (imprecision and/or uncertainty). Thus, a special attention should be paid. In our approach, we chose the probabilistic-possibilistic transformation, because this technique perfectly manipulates most of the imperfections related to our biometric data without loss of relevant information. Besides, these transformations are useful especially when dealing with uncertain and imprecise information.

Many techniques have been developed to obtain a possibility distribution based on the probability distribution [20]-[23]. They can be classified into two categories of probability-possibility transformations; one is based on the precise probability value and the other on the probability interval. The choice of the method and the class of probability-possibility transformation, meeting the requirements of our iris modality, is a crucial step in our work. Variability and ambiguity, present in our iris data, make it difficult to get an accurate probability value. Thus, the obtained possibility distribution may not be satisfactory. To overcome this limitation, the probability confidence intervals offer an accurate tool for modeling such imperfections. Accordingly, the probabilistic-possibilistic transformation of Campos and Huete [24], relying on the probability intervals, is more able to cope with collected biometric data imperfections.

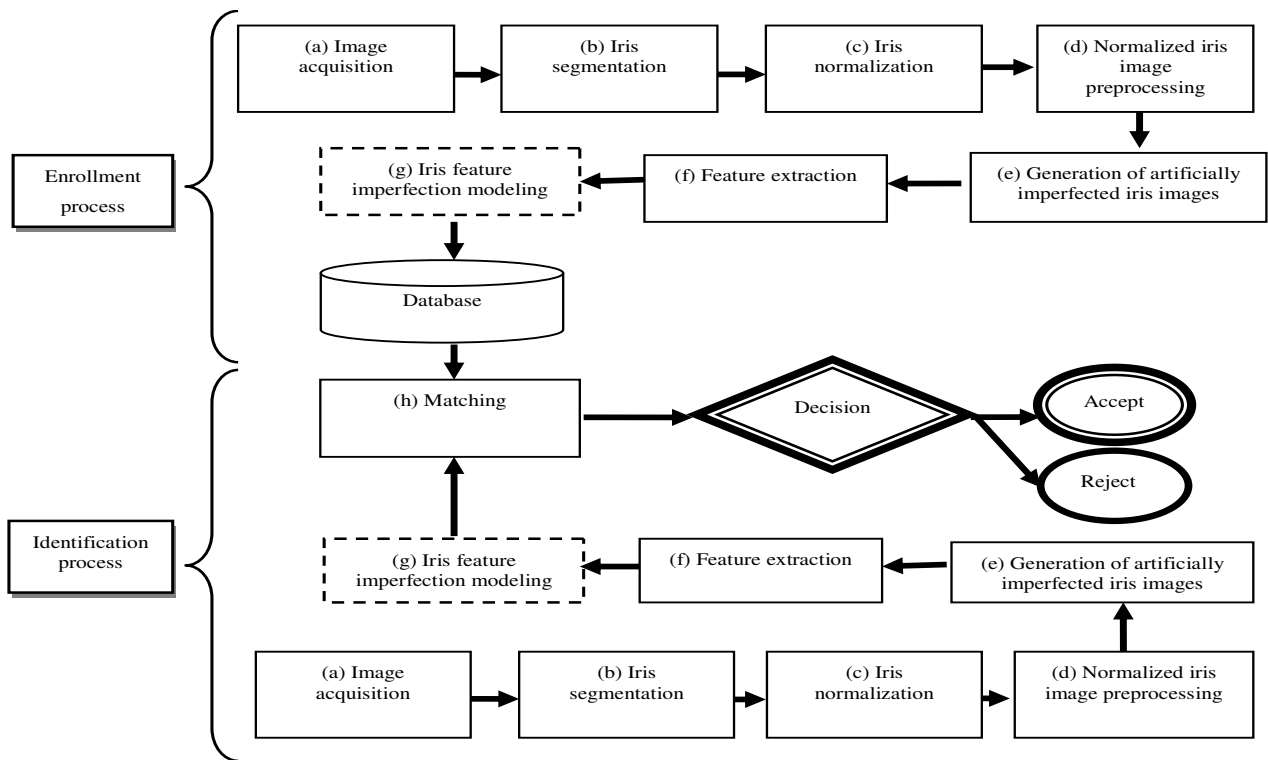


Fig 1: Flow of the proposed iris recognition system: (a) image acquisition; (b) iris segmentation; (c) iris normalization; (d) normalized iris image preprocessing; (e) generation of artificially imperfed iris images; (f) feature extraction; (g) iris feature imperfection modeling; (h) matching.

An iris recognition system can be efficient if it is applied to a specific database but gives unsatisfactory results when applied to another database. By modeling the imperfection information contained in the extracted iris feature with the uncertainty theories, we hope to have a generic and performing iris system despite the errors that may occur during the acquisition or segmentation of the iris and the used normalization or extraction method.

In this paper, we propose an improved approach essentially based on iris feature imperfection modeling process. This modeling step is divided into four stages: In the first stage, the extracted feature is transformed into normalized measurements by Z-score and Min-Max normalization methods [25]. In the second step, the normalized feature is transformed into histogram probability distribution based on histogram parameters [26]. In the third step, the histogram probability distribution is transformed into interval probability distribution using Goodman formalism [27]. Finally, in the fourth step, the interval probability distribution is transformed into possibility distribution relying on Campos and Huete approach [24]. For the matching process, a similarity measure based on Manhattan distance is applied. Different experiments are performed on two subsets of CASIA-V4 iris image database to assess the proposed system. The purpose of our study is to apply the uncertainty theories for overcoming iris-data biometric system imperfections.

The remainder of this paper is organized as follows: section 2 presents a detailed description of the basics of non typical proposed iris recognition systems taking into account data imperfections. In this section, we involve all the steps of a typical iris recognition scheme including the proposed iris feature imperfection modeling approach. Section 3 provides the experimental results performed on two subsets of CASIA-V4 iris image database. Then, the performance of the proposed system is discussed and compared to a typical iris recognition system from the state-of-the-art. Conclusions of this present work are finally drawn in section 4.

2 Proposed iris recognition system

Starting with typical solutions of iris recognition, we try in this section to adapt the different processing steps for an adequate representation of iris images taking into account some artificially introduced imperfections. Accordingly, details of the proposed system are given.

An iris system consists of an enrollment process and identification one (Fig. 1). The enrollment phase is the process of capturing information on the subject and storing them in a database. It consists of image acquisition, iris segmentation, iris normalization, normalized iris image preprocessing, generation of artificially imperfedted iris images, feature extraction and finally iris feature imperfection modeling. In a first learning step, these features are stored as signatures in a database. The identification process compares the request input iris signature to stored ones, by a matching process for making a decision (accept or reject).

In order to achieve a robust iris recognition system, it is necessary to establish some coherent steps. Our proposed system consists of eight steps that can be described as follows:

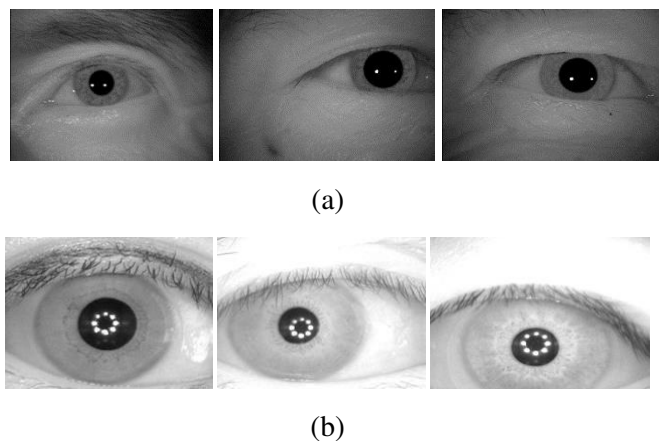


Fig 2: Samples of eye images : (a) CASIA-V4-Synthetic database; (b) CASIA-V4-Interval database.

2.1 Image acquisition

It is a major process aspect of the iris recognition system and consists in image acquisition. The iris images used in this research are provided by the biometrics research team at the Center Biometrics and Security Research (CBSR), National Laboratory of Pattern Recognition (NLPR) and the Institute of Automation, Chinese Academy of Sciences (CASIA). CASIA-V4 is public and contains six subsets. It is actually used to evaluate the performance of iris recognition systems [28].

To evaluate the proposed system, we selected two subsets of CASIA-V4 iris image database namely Interval and Synthtetic [29]. The reason of this choice is first to assess the robustness of the proposed approach. In addition, we tried to examine the effectiveness of our method dealing with different cases of non-ideal iris images. Some samples of images in each database are presented in Fig. 2. Finally, this selection may help to evaluate the efficiency of the proposed method in overcoming many problems faced in the iris localization, and feature extraction or matching process, leading to some types of imperfections. In the following, a brief description of the databases was provided:

- The CASIA-V4-Synthtetic database contains 10,000 iris images from 1,000 subjects. This database contains images with different visual qualities: some images seem perfect whereas others are noisy or blurry due to adverse illuminations. The main causes of intra-class variations in this

database are hair presence, eyelid and eyelash obstruction, iris images included rotation and deformation. Some iris samples from this database are illustrated in Fig. 2 (a).

- The CASIA-V4-Interval database contains 2639 iris images from 249 subjects. The subjects attributes are captured from students (Fig. 2 (b)). The captured iris images are very clear. This database is well suited for studying the detailed texture feature of iris images.

2.2 Iris segmentation

This step is very important in any recognition system, it has a direct influence on the performance of the system. A good segmentation consists in perfectly extracting the iris texture region from the eye. The proposed method is based on two steps (Fig. 3): segmentation technique by classification of pixels to detect the pupil followed by a morphological cleaning and as a result the detection of the internal contour of the iris. The detection of the external contour of the iris region and the contours of eyelids is carried out by a multi-scale analysis technique, based on Mallat and Zhong wavelet [30], proposed by Nabti and Bouridane [31] in the second step. These both steps are detailed as follows.

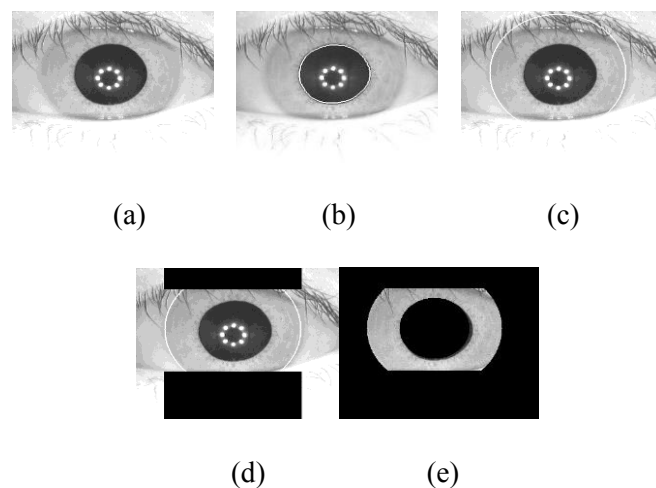


Fig 3: Steps of iris segmentation : (a) eye image ; (b) iris internal contour detection ; (c) iris external contour detection; (d) eyelid contour detection; (e) iris localization.

Let $f(x,y)$ be an image of size $M \times N$.

Step 1 : Iris internal contour detection

The internal contour of the iris corresponds to the contour of the pupil. To delimit the iris in the interior, the pupil has to be accurately located. This region of the human eye has the particularity to be the darkest object in the image, which helps in its location process. Besides, the distinguished form of the pupil, often approximated by a disc or ellipse, could help in the detection of its contour.

In this first step, we propose an effective and appropriate method for the two selected subsets of CASIA-V4 iris image database. The proposed method is included within the framework of segmentation techniques by pixels classification and it consists in two stages: one for the localization of the pupil and the second for a morphological cleaning of the image outcome from the first step. The pixels, which are strictly less than a variable β corresponding to the pupil belong to a class whereas the rest of the image pixels have another class. The β value depends on the illumination system used for image acquisition. Then, Eq. 1 is applied to generate a binary image I_{bin} , where the white object is the pupil (Fig. 4 (b)).

$$I_{bin}(x,y) = \begin{cases} 1 & \text{if } f(x,y) < \beta \\ 0 & \text{else} \end{cases} \quad (1)$$

The binary image I_{bin} may be blurred by holes in the region defining the pupil due to reflection points resulting from the acquisition step. There may also be cases where the eyelashes or eyebrows appear as dark as the pupil, resulting in their inclusion in the I_{bin} image. To overcome this disadvantage, a cleaning of the image is performed relying on morphological operators: a dilation followed by an erosion (closing operation), and an erosion followed by a dilation (opening operation) again:

- The closing event aims to get rid of all small sized elements. This procedure proved to be very useful to fill the points of reflection that appear in the pupil (Fig. 4(c)).
- The opening operation, however, can eliminate all the parts of the objects that do not contain the structuring element. The application of this procedure on the I_{bin} image can eliminate the eyelashes and eyebrows that appeared in most of the tested cases (Fig. 4 (d)).

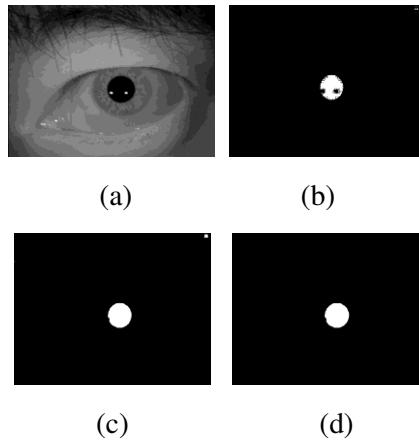


Fig 4: Steps for the detection of the internal contour of the iris:(a) eye image; (b) binary image I_{bin} (c) closing of the binary image I_{bin} ; (d) opening of the binary image I_{bin} .

When the pupil is localized successfully in the image, we can reach a circular object and determine its characteristic parameters. Indeed, with such an approximation, the geometric center coincides with the gravity center [32], whose coordinates are given by:

$$i_u = \frac{1}{u} \sum_{I_{bin}(x,y) \in U} i \quad (2)$$

$$j_u = \frac{1}{u} \sum_{I_{bin}(x,y) \in U} j \quad (3)$$

Where u is the number of pixels forming the pupil and (x,y) are the coordinates of a pixel belonging to U . Given that the sum of the pixels forming the pupil defines the surface S , the radius may be given by:

$$R_u = \sqrt{\frac{S}{\pi}} \quad (4)$$

The center of the pupil is not necessarily in the center of the iris, but it is very useful in the extraction of its external contour.

Step 2: Iris external contour and eyelid contour detection

In this second step, the detection of the external contour of the iris region and the contours of eyelids is undertaken by a multi-scale analysis technique [30], [31]. This consists essentially on calculating the gradient of the image at different scales. All the filters used to scale j ($j > 0$) are over-sampled by a factor of

2^j compared to those in the zero scale. In addition, the smoothing function used in the construction of a wavelet reduced the effect of noise. Thus, the smoothing step and the contour detection are combined together to achieve an optimal result. This is the essential criterion that prompted us to use the multi-scale analysis in this work.

Our detection method is based on the multi-scale analysis via wavelet Mallat and Zhong [30]. In order to use this technique, we opted for a dyadic wavelet transform "quadratic spline" whose Fourier transform is:

$$\widehat{\Psi}(\omega) = i. \omega \left(\frac{\sin(\frac{\omega}{4})}{\frac{\omega}{4}} \right)^4 \tag{5}$$

with i the complex number null real and imaginary unitary.

The dyadic wavelet transform is a particular class of the wavelet families, characterized by the fact that the daughters wavelets are derived from the mother wavelet by a sequence of sampled levels according to a sequence 2^j . For our application, we make use five scales. At each level, with $(j > 0)$, the wavelet transform decomposed $(S_{j-1}f)$ into three bands of wavelets:

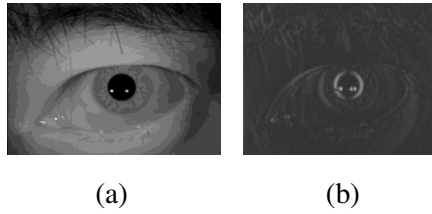


Fig 5: Contour map used for the detection of the external contour of the iris: (a) eye image; (b) vertical details sequence (2^4).

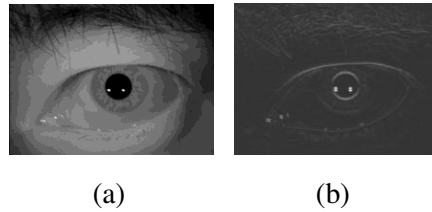


Fig 6: Contour map used for the detection of the contours of the eyelids: (a) eye image; (b) horizontal details sequence (2^4).

- The approximation band $(S_j f)$, due to a low pass filter. The filter form is given by :

$$F'(\omega) = e^{i\frac{\omega}{2}} \left(\cos(\frac{\omega}{2}) \right)^{2n+1} \tag{6}$$

For the scale j we have the equation:

$$S(x, y, j + 1) = S(x, y, j) * (F_j^d, F_j^d) \tag{7}$$

- The horizontal details band, noticed $W_j^H f$, and the vertical details band, noticed $W_j^V f$, : due to a high pass filter. The filter form is given by :

$$F''(\omega) = 4. i. e^{i\frac{\omega}{2}} \left(\sin(\frac{\omega}{2}) \right) \tag{8}$$

For the scale j we have the equations:

$$W_j^H f(x, y, j) = \frac{1}{\lambda_j} S(x, y, j) * (D, F_j^d) \tag{9}$$

$$W_j^V f(x, y, j) = \frac{1}{\lambda_j} S(x, y, j) * (F''^d_j, D) \tag{10}$$

with F_j^d and F''^d_j the filters kernel, respectively high and low at a scale j . D is a Dirac impulsion. (*) corresponds to the convolution product; j is a factor that compensates the discretization effect.

Once generated, the vignettes $W_j^H f$ and $W_j^V f$ serve as contour maps. Retaining only the items with maximum local amplitudes, we see that the vertical details to scale ($j=4$), give a better lateral discrimination to the external contours of the iris (Fig. 5), whereas the horizontal details used to scale ($j=3$) give a better discrimination of the contours of the eyelids (Fig. 6). The Circular Hough transform was used to search the radius of the iris external contour, the center being previously fixed assuming that the iris and the pupil are concentric.

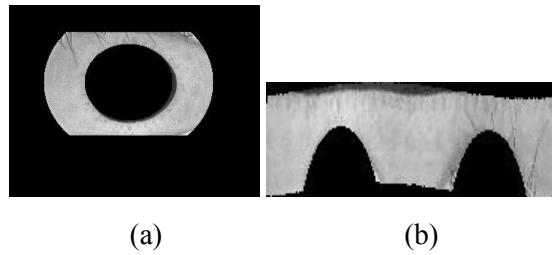


Fig 7: Iris normalization: (a) iris image localized; (b) iris image normalized

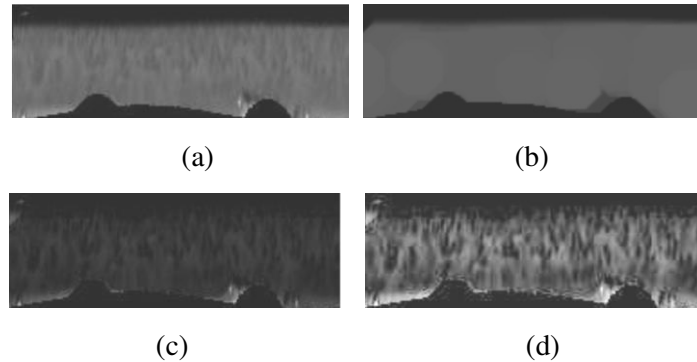


Fig 8: Iris pre-processing steps: (a) original image; (b) background computed; (c) image with uniform illumination; (d) image with enhanced contrast.

2.3 Iris normalization

In this step, Daugman's method [33] was applied for iris normalization. Daugman's transformation is commonly adopted since it easily deals with dilatation or contraction of the pupil (Fig. 7). This model consists in unrolling linearly the crown which presents the iris in the image. It corresponds to the passage from the cartesian coordinate system to the polar coordinate system:

$$I(x(r, \theta), y(r, \theta)) \rightarrow I(r, \theta) \tag{11}$$

Daugman's pseudo polar transformation consists in defining $x(r, \theta)$ and $y(r, \theta)$ as linear combinations of the points between $(x_p(\theta), y_p(\theta))$ located on the iris-pupil contour to a direction θ and the point $((x_i(\theta), y_i(\theta))$ located on the iris-sclerotic contour with the same direction. The equations used for this conversion are as follows:

$$x(r, \theta) = (1 - r).x_p(\theta) + r.x_i(\theta) \tag{12}$$

$$y(r, \theta) = (1 - r)y_p(\theta) + r.y_i(\theta) \quad (13)$$

where each point within the iris region is transformed into a pair of polar coordinates (r, θ) , r is on the interval $[0, 1]$ and θ is an angle on the circle $[0, 2\pi]$.

In the new polar coordinate system, clearing any movement that is horizontal, vertical or even the combination of both, needs to take the center of the pupil as a reference point. The values of these radial and angular resolutions present the new image height and width, respectively.

2.4 Iris pre-processing

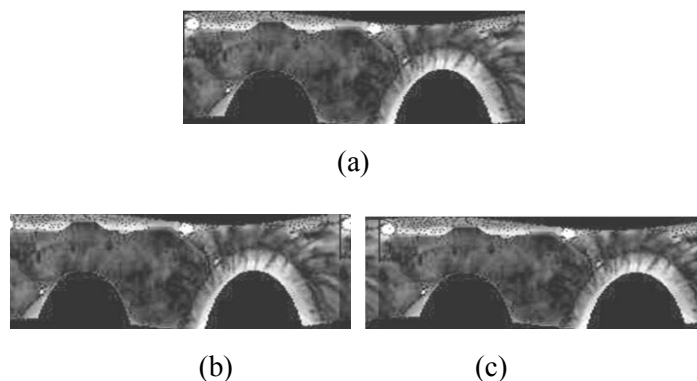


Fig 9: Artificially imperfected normalized iris images: (a) original image; (b) artificially imperfected image ;(c) artificially imperfected image

To extract more discriminative feature, it is necessary to correct the irregular illumination and adjust the intensity values for contrast enhancement from a normalized iris image. Thus, the opening morphological operation was used to level out the lighting in the image and a contrast limited adaptive histogram equalization (CLAHE) [34] to enhance the contrast of each small region in the image, called tiles, and combine the neighboring tiles using bilinear interpolation to eliminate artificially induced boundaries. The preprocessing process of the normalized iris image (Fig. 8) is detailed in the following paragraph.

Firstly we use an opening morphological operation to estimate the background of the iris image (Fig. 8 (b)). Secondly, we subtract the estimated background from the original image to obtain an image with a uniform illumination (Fig. 8 (c)). We end up by applying the CLAHE histogram on the same image processed (Fig.8(d)).

2.5 Generation of artificially imperfected iris images

In real applications, normalized iris images are usually affected by some types of imperfections, such as variability, ambiguity, incompleteness, etc. A very simple idea to cope with such imperfections is to use a large amount of registered samples. However, we cannot usually get enough registered samples. In this context, generating artificially imperfected images by all potential kinds of imperfections can be applied for more effectiveness. We accordingly generate imperfected images from original normalized iris images.

The process of generation of artificially imperfected iris images is achieved by the circular shift method applied to each normalized iris image with different positions. Some artificially imperfected iris images are shown in Fig. 9. The equation used for this generation is as follows:

$$f'' = \text{circshift}(f', t) \quad (14)$$

where $f'(x,y)$ is an original normalized iris image, $f''(x,y)$ is the artificially imperfedted iris image and (t) is the shift number.

2.6 Feature extraction

The purpose of this step was the extraction of relevant information that characterizes each individual. The vector containing this information is called signature. Generally, an iris signature is generated following its texture analysis, which is the most relevant. The approach used here is also given by Khanfir in [35] for iris extraction. This feature extraction technique is based on a box-counting fractal dimension [36], incorporating a characterization of the iris texture.

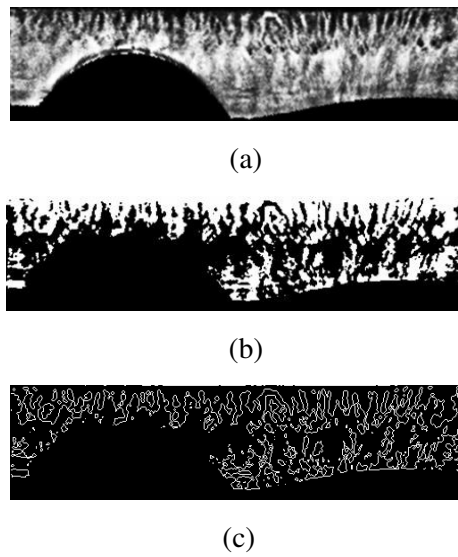


Fig 10: Steps of determining the contour map for fractal analysis: (a) original image; (b) binary image; (c) map feathering contours of the primitive of the iris texture.

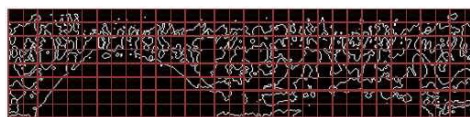


Fig 11: Division the image of the iris texture into 256 blocks.

A box-counting fractal dimension is commonly used in practical situations to compute the fractal dimension of an image owing to its simplicity and easy implementation. The process consists on covering iteratively an artificially imperfedted iris image (f'') by a grid of uniformly sized squares. (B_c) is the side length of the square, $e(B_c)$ is the number of boxes containing the information in the image. The box-counting dimension is defined as follows:

$$D(f'') = \lim_{B_c \rightarrow 0} \frac{\log(e(B_c))}{\log(1/B_c)} \quad (15)$$

After transforming the artificially imperfedted iris image into a binary image, the extraction approach proposed by Khanfir [35] consists on quantifying the evolution of the roughness of the texture within the iris and its fragmentation in its polar landmark (Fig. 10). This is quantified by computing the local fractal dimensions on the contour map fragments of the iris texture. Indeed, we divide the image of the iris texture

into 256 blocks ($B_c=16$ pixels), and then compute the fractal dimension of each block (Fig. 11). Thus a vector containing 256 elements is recovered.

2.7 Iris Feature imperfection modeling (proposed approach)

Our modeling process is divided into four steps. They are detailed in the following subsections.

2.7.1 Extracted feature normalization

Normalization of the biometric data [37] is generally performed to remove unwanted impurities. However, in this case, when performing normalization, the statistical property for each set of data has also been taken into consideration prior to the probabilistic-possibilistic transformation process. In our work, the normalization step was divided into two stages. These stages are as follows:

Stage1 : Z-score method normalization

The Z-score normalization technique [25] allows for a very straight elimination of systematic errors and drifts. It is computed using the arithmetic mean and standard deviation of the given biometric data. The normalized raw measurements M_N of each feature of each individual class are given by [25] :

$$M_N = \frac{M_R - \mu}{\sigma} \quad (16)$$

Where M_R is the raw measurements, μ is the arithmetic mean and σ is the standard derivation of the given measurements. The drawback of this method is that it does not ensure a common interval for our normalized feature. Thus, we sought to apply a second normalization on these biometric data to establish them in a common interval.

Stage 2 : Min-Max method normalization

The Min-Max normalization technique retains the original measurements on a near scale factor and transforms all the measurements in the interval $[0,1]$. The normalized raw measurements M'_N are given by :

$$M'_N = \frac{M_N - \min(M_N)}{\max(M_N) - \min(M_N)} \quad (17)$$

Where M_N is the first normalized raw measurements.

2.7.2 Transformation of the normalized feature into histogram probability distribution

The histogram is the most important graphical tool for trading data distribution. It gives an idea of how frequently data in each class occurs in the training data set. In our work, we used histogram parameters [38], [26], for each feature of each individual class, to get a histogram probability distribution. This step was divided into two stages:

Stage1 : Transformation of the normalized feature into data histogram

The histogram is computed in the following way: an interval $(z_2 - z_1)$ of a feature is divided into k subintervals of equal length; each subinterval is called h . We do not know the probability distribution function. Therefore z_1 and z_2 are determined as either the minimal and maximal values of the data set according to each feature [38]. The h width thus is defined by :

$$h_{\text{width}} = \frac{z_2 - z_1}{k} \quad (18)$$

Accordingly, the normalized feature is transformed into data histogram H with $H = \{h_i, i=1,2,\dots,k\}$.

Stage 2 : Transformation of the data histogram into histogram probability distribution

The height of h_i is determined by computing the number n_i of occurrences of the data patterns within the interval of this h . The probability p_i assigned to h_i is the ratio of h height to the total number n of patterns :

$$p_i = \frac{n_i}{n}; i = 1,2, \dots, k \tag{19}$$

Using Eq. 19, the data histogram H is transformed into histogram probability distribution p with $p=\{p_i; i=1,2,\dots,k\}$.

2.7.3 Transformation of the histogram probability distribution into interval probability distribution

A classical approach for deriving a possibility distribution from our biometric data is to transform the histogram probability distribution P and to apply Dubois and Prade transformation [21] relying on precise-valued probabilities. However this approach does not into account the uncertainty. The confidence intervals are a usual means to estimate the unknown parameters of a probability distribution. A confidence interval on a parameter at a given level α is an interval that contains the true value of the parameter with probability $1-\alpha$.

In this third modeling step, we estimate the histogram probability distribution P using simultaneous confidence intervals on multinomial proportions, and then to derive a possibility distribution from this interval probability distribution. In our work, the multinomial proportion applied with the parameter $P=\{p_i; i=1,2,\dots,k\}$ is the histogram probability distribution.

Suppose that the available data we have in the sample space $\Omega = (\omega_1, \omega_2 \dots \omega_k)$ consists of n observations divided into k classes. n_i denotes the number of observations falling in the i^{th} class ω_i in a data of size n , then $M_d = (n_1, n_2, \dots, n_k)$ as a multinomial proportion with parameter $P = (p_1, p_2, \dots, p_k)$, where each $p_i = p_r (\{\omega_i\}) > 0$ is the probability p_r of the i^{th} class and $\sum_{i=1}^k p_i = 1$.

There has been a great deal of research on the construction of the simultaneous confidence intervals for a multinomial proportions [39],[40]. In our work, we applied the method proposed by Goodman detailed in [27] to transform the histogram probability distribution into interval probability distribution. This technique is very fast compared to another efficient method developed by Sison and Glaz in [40]. It is also one of the most widely used techniques in practical situations [27]. The main formulas are given as follows:

Let A, B_i, C_i and Δ_i be constants given by Eqs. 20 to 23 where $\chi^2(1 - \frac{\alpha}{k}, 1)$ denotes the quantile of order $1 - \frac{\alpha}{k}$ of the chi-square distribution with one degree of freedom, where k represents the number of probability intervals and $n = \sum_{i=1}^k n_i$ denotes the size of the data(or sample).

$$A = \chi^2(1 - \frac{\alpha}{k}, 1) + n \tag{20}$$

$$B_i = \chi^2(1 - \frac{\alpha}{k}, 1) + n_i \tag{21}$$

$$C_i = \frac{n_i}{n} \tag{22}$$

$$\Delta_i = B_i^2 - 4AC_i \tag{23}$$

Thus Goodman's intervals with confidence level of $(1- \alpha)$ are defined as follows:

$$[p_i^-, p_i^+] = \left[\frac{B_i - \Delta_i^{1/2}}{2A}, \frac{B_i + \Delta_i^{1/2}}{2A} \right]; i = 1,2, \dots, k \tag{24}$$

Using Eq. 24, the histogram probability distribution P is transformed into interval probability distribution I with $I = \{[p_i^-, p_i^+]; i = 1,2,\dots,k\}$.

2.7.4 Transformation of the interval probability distribution into possibility distribution

A consistency principle between probabilities and possibility was first stated by Zadeh [11] in an unformal way: what is probable should be possible. In the literature, several transformations from probabilities to possibilities have been proposed. In particular, Campos and Huete method [24] produces the most specific possibility distribution among the ones dominating a given probability distribution. In this step, the interval probability distribution I is transformed into possibility distribution Π relying on the fast and efficient approach proposed by Campos and Huete [24]. This method is elaborated for generalizing the Dubois and Prade probabilistic-possibilistic transformation procedure [23] based on probability intervals.

Consider the events $E=(x_1, x_2, \dots, x_k)$, $x_i \in E$ with $i=1, \dots, k$ and $E \subseteq \Omega$. For each event x_i , a confidence intervals I of possible values for p_i with $(p_i^- < p_i^+)$ are given, also let k_i be the greatest index verifying $(k_i < i)$ and $(p_{k_i}^- > p_i^+)$. If such a k_i does not exist, we consider $k_i=0$. The equation of the probability-possibility transformation is defined by the means of :

$$\pi_i = \min \left(\left(1 - \sum_{j=1}^{k_i} p_j^- \right), \left((i - k_i) p_i^+ + \sum_{j=i+1}^k p_j^+ \right) \right), \text{ where by definition } \sum_{j=1}^{k_i=0} p_j^- = 0 \quad (25)$$

Using Eq. 25, the interval probability distribution I is transformed into coherent and consistent possibility distribution π , with $\pi = \{\pi_i; i=1, 2, \dots, k\}$.

2.8 Matching

Any decision for identification purposes leads us to a measure of dissimilarity between the stored characteristics and the given ones. Let d be any distance between two iris signatures, whether acquired by the same person or by two different individuals. In our work, the feature extracted from the iris of each individual are transformed into possibility distribution.

In this matching step each iris signature is compared to other iris representations stored in a database in order to make a decision. Accordingly, a similarity measure should be applied to find out similar possibility distributions. To estimate the similarity measures between two iris signatures [20], several measures such as Manhattan distance, Information Affinity distance, Euclidean distance and others can be used. In our approach, to carry out such an estimation between two possibility distributions of iris signatures, we relied on the normalized Manhattan distance.

Let π_1 and π_2 be two normalized possibility distributions on the same universe of discourse $\Omega=(\omega_1, \omega_2, \dots, \omega_k)$, this normalized Manhattan distance is given by:

$$d_M(\pi_1, \pi_2) = \frac{1}{k} \sum_{i=1}^k |\pi_1(\omega_i) - \pi_2(\omega_i)| \quad (26)$$

This distance measure can be transformed into a similarity measure to compare the possibility distributions as follows:

$$S_M(\pi_1, \pi_2) = 1 - d_M(\pi_1, \pi_2), \text{ where } S_M \text{ is a similarity measure.} \quad (27)$$

3 Results and discussion

In order to have a baseline for the comparison of the achieved results of the proposed method, we compared our iris recognition system to a typical one [35]. This biometric system consists of almost the same steps and methods as our proposed system, except for the iris feature imperfection modeling step (Fig. 1 (g)) which was omitted and the decision stage (Fig. 1 (f)) is achieved relying on the normalized Manhattan distance.

In order to compare the proposed iris recognition system and that of the typical system [35], we extracted a subset of image samples from the CASIA-V4-Interval iris image database, including 700 left eye images of 100 subjects, having therefore 7 images per eye, whereas, for the CASIA-V4-Synthetic iris image database, we used all images of this database which contains 1000 subjects and 10,000 iris images. In our experiments, the EER, AUC and finally the ARR statistics were computed and used for the performance assessment of both proposed and typical [35] systems. In our experiments, it is proposed to give the corresponding rate only to the testing phase.

A first experiment to assess performance of the proposed iris system was conducted with a subset of right eye image samples from the CASIA-V4-Interval iris image database. The AUC, EER and ARR were used to assess the overall performance of both systems. The results of these assessments are shown also in Table 1. These outcomes confirm the improved performance yielded by the proposed system compared to the typical one [35] and indicating the feasibility of an iris recognition using a modeling iris feature step based on uncertainty theories.

CASIA-V4-Interval (100 subjects, 700 images)	Typical system (without proposed approach)	Proposed system (with proposed approach)
AUC	0.8647	0.9999
EER(%)	21.3	0.06
ARR(%)	78.69	99.93

Table 1: AUC, EER and ARR obtained for both systems on a subset of left eye image samples from CASIA-V4-Interval iris image database.

Following the encouraging results obtained in the first experiment using the step of modeling imperfections iris feature and applied on a CASIA-V4-Interval iris image database, additional experiments were also conducted on CASIA-V4-Synthetic iris image database to assess the performance of our proposed iris system. Tables 2 give the values in terms of AUC, EER, and ARR for this database. The results obtained in this table demonstrate the recognition efficiency of the proposed biometric system.

CASIA-Synthetic (1000 subjects, 10 000 images)	Proposed system (with proposed approach)
AUC	0.9999
EER(%)	0.14
ARR(%)	99.86

Table 2: AUC, EER and ARR obtained for the proposed system on CASIA-V4-Synthetic iris image database.

Table 3 and table 4 show the comparison between our proposed method and others methods [39]-[47] tested with samples iris images from CASIA-V4-Interval database, CASIA-V4-Synthetic iris image database and CASIA-V1 database. Observing the values on the tables, we can see that the AUC and ARR of the proposed method significantly exceed the AUC and ARR of other methods in most of the cases. It is also noticed that the lower EER value are provided by the proposed method over the others. Therefore, we can assume that our method perfectly minimizes the recognition errors.

CASIA V4-Interval	Daugman method [41] (2015, 500 images)	Mira and al method [41] (2015,500 images)	Saminathan and al method [42] (2015)	Rathgeb and al. method [43] (2016)	Proposed method (700 images)
AUC	0.9976	0.9975	-	-	0.9999
EER(%)	1.05	1.12	-	0.98	0.06
ARR(%)	98.95	98.88	98.5	-	99.93

Table 3: Comparison between our proposed method and others methods applied on CASIA V4-Interval

Authors, year	Database, subjects, images	ARR(%)
Rai and al [44], 2014	CASIA-V1, 108 ,756	99.91
Abiyev and al [45], 2008	CASIA-V1, 108 ,756	99.25
Ali and al [46], 2008	CASIA-V1, 108 ,756	100
Proposed method	CASIA-V4-Synthetic,1000, 10.000	99.86

Table 4 : Comparison between our proposed method and others methods applied on CASIA-V1 and CASIA-V4-Synthetic

4 Conclusions

The main goal of our work was to build a robust iris recognition system to solve the new difficulties faced in this area. We are not trying to build a new method of localization of iris or an efficient extraction method of relevant information because, from the literature, we have seen that the performance of these methods varies according to the quality of the iris image. For this reason, we have chosen to treat imperfect information. The results show that our proposed system based on the uncertainty theories improves robustness and reliability in terms of identification and the proposed iris feature imperfection modeling approach was very effective in treating the imperfections found in the iris signature. Our contribution has consequently improved the performance of the typical iris recognition system [35].

In this paper, we proposed a robust method for iris recognition system based on the uncertainty theories. The experimental results on two subsets of CASIA-V4 iris image database namely: Synthetic and Interval, show that the identification performance of the proposed system is improved, compared to other typical iris recognition system. It proves the robustness of our approach dealing with some imperfections related to the iris biometric data. It should be noted that in the present work, our aim was to improve the performance of a recognition system regardless the use of ideal and/or non-ideal iris images from the database, or the imperfections that appear in the extracted iris feature.

References

- [1] J. G. Daugman, "Biometric Personal Identification System Based on Iris Analysis", United States Patent, no.5291560, 1994.
- [2] S.Thainimit, C. Sreecholpech, V. Areekul and C. H. Chu, "Robust Iris Segmentation Based on Local Image Gradient Properties," *IEICE Trans. Inf. & Syst.*, vol. E94-D, no. 2, pp. 349-356, Feb. 2011.
- [3] P. Li, X. Liua, L. Xiaoa, and Q. Songa, "Robust and Accurate Iris Segmentation in Very Noisy Iris Images," *Image and Vision Computing*, vol.28, no.2, pp. 246–253, 2010.

- [4] J. Sun, L. Zhou, Z. Lu and T. Nie, "Iris Recognition Based on Local Gabor Orientation Feature Extraction," *IEICE Trans. Inf. & Syst.*, vol. E98-D, no. 8, pp. 1604-1608, Aug. 2015.
- [5] S. Noh, K. Bae, K. R. Park and J. Kim, "A New Iris Recognition Method Using Independent Component Analysis," *IEICE Trans. Inf. & Syst.*, vol. E88-D, no. 11, pp. 2573-2581, Nov.2005.
- [6] T. Mina and R. Parka, "Eyelid and Eyelash Detection Method in the Normalized Iris Image Using the Parabolic Hough model and Otsu's Thresholding Method," *Pattern Recognition Letters*, vol. 30, no. 12, pp. 1138–1143, 2009.
- [7] H. Takano, H. Kobayashi, and K. Nakamura, "Rotation Invariant Iris Recognition Method Adaptive to Ambient Lighting Variation," *IEICE Trans. Inf. & Syst.*, vol.E90-D, no. 6, pp. 955–962, Jun. 2007.
- [8] P. Grother, J. R. Matey, E. Tabassi, G. W. Quinn, M. Chumakov, "IREX VI: Temporal Stability of Iris Recognition Accuracy (Iris Ageing)," *NIST Interagency Report 7948*, July. 2013.
- [9] S. H. Moi, H. Asmuni, R. Hassan, R. M. Othman, "Multimodal Biometrics:Weighted Score Level Fusion Based on Non-ideal Iris and Face Images," *Expert Systems with Applications*, vol. 41, no.11, 2014.
- [10] A.Motro and P. Smets, eds., *Uncertainty Management in Information Systems*, Springer Science and Business Media New York, 1997.
- [11] L. A. Zadeh, "Fuzzy Sets," *Information and Control*," vol. 8, pp. 338-353, 1965.
- [12] G. A. Shafer, ed., *Mathematical Theory of Evidence*, Princeton Univ. Press, 1976.
- [13] D. Dubois and H. Prade, eds., *Possibility Theory: An Approach to Computerized Processing of Uncertainty*, Plenum Press New York, 1988.
- [14] L. A. Zadeh, "Fuzzy Sets as a Basis for a Theory of Possibility," *Fuzzy Sets and Systems*, vol. 100, no. 1, pp. 9-43, 1999.
- [15] G. Cooman and D. Aeyels, "A Random Set Description of a Possibility Measure and its Natural Extension," *IEEE Trans. on Syst, Man and Cybernetics*, vol. 30, no. 2, pp. 124-130, 2000.
- [16] D. Dubois, D. Cayrac and H. Prade, "Handling Uncertainty with Possibility Theory and Fuzzy Sets in a Satellite Fault Diagnosis Application," *Proc. 6th Int. Conf. on Information Processing and Management of Uncertainty in Knowledge Based Systems*, vol. 4, no. 3, pp. 251-269, 1996.
- [17] J. Frikha, D. Sellami, and I. Khanfir Kallel, "Indoor/outdoor navigation system based on possibilistic traversable area segmentation for visually impaired people," *ELCVIA Electron. Lett. Comput. Vis. Image Anal.*, vol. 15, no. 1, p. 60, Aug. 2016.
- [18] Bellaaj M., Masmoudi D. S and Kallel I. K., "Possibilistic Modeling of Iris System for High Recognition Reliability", *IJCSNS International Journal of Computer Science and Network Security*, Thomson Reuters Publishing, Volume Number: Vol.16, No.7, pp.34-47, *July. 2016*.
- [19] M. Bellaaj, J. F. Elleuch, D. S. Masmoudi and I. K. Kallel, "An Improved Iris Recognition System Based on Possibilistic Modeling," *Proc. 13th Int. Conf. on Advanced in Mobile Computing and Multimedia (MoMM)*, Brussels, Belgium, pp. 26-32, Dec. 2015.
- [20] I.Jenhani, "From Possibilistic Similarity Measures to Possibilistic Decision Trees", thesis for obtaining the PhD from the University of Artois, French, 2010.
- [21] D.Dubois, H.Prade and S.Sandri, "On Possibility/probability Transformations," in *Theory and Decision Library*, eds. W. Leinfellner, G. Eberlein, R. Lowen, vol. 12, pp. 103-112, 1993.
- [22] M. Masson and T. Denoeux, "Inferring a Possibility Distribution from Empirical Data," *Fuzzy Sets and Systems*, vol. 157, no. 3, pp. 319-340, 2006.
- [23] D.Dubois and H. Prade, "Représentations Formelles de l'Incertain et de l'Imprécision," in *Concepts et Méthodes pour l'Aide à la Décision*, ed. Hermes-Lavoisier, vol. 1, pp. 111-165, Lavoisier S.A.S., 2006.
- [24] L. M. Campos and J. F. Huete, "Measurement of Possibility Distributions," *Int. J. General Systems*, vol. 30, no. 3, pp. 309–346, 2001.

- [25] F. Alsade, N. zaman, M. Z. Dawood and S. H. A. Musavi, "Effectiveness of Score Normalisation in Multimodal Biometric Fusion," *Journal of ICT*, vol. 3, no. 1, pp. 29-35, 2009.
- [26] M. S. Mouchaweh and P. Billaudel, "Influence of the Choice of Histogram Parameters at Fuzzy Pattern Matching Performance", *WSEAS Transactions on Systems*, vol. 1, no. 2, pp. 260-266, 2002.
- [27] L. A. Goodman, "On Simultaneous Confidence Intervals for Multinomial Proportions," *Technometrics*, vol. 7, no. 2, pp. 247–254, 1965.
- [28] F. He, Y. Liu, X. Zhu, C. Huang, Y. Han and H. Dong. "Multiple Local Feature Representations and their Fusion based on an SVR Model for Iris Recognition using Optimized Gabor Filters," *EURASIP Journal on Advances in Signal Processing*, 2014.
- [29] 2010 TNT Group, "CASIA-IrisV4 collected by CASIA", Institute of Automation, Chinese Academy of Sciences, <http://biometrics.idealtest.org/>, accessed Janv. 5. 2016.
- [30] S. Mallat and S. Zhong, "Characterization of Signals from Multiscale Edges," *IEEE Trans. on Pattern Analysis and Machine Intelligence*, vol. 14, no. 7, pp. 710-732, 1992.
- [31] M. Nabti and A. Bouridane, "an Effective and Fast Iris Recognition System based on a Combined Multiscale Feature Extraction Technique," *Pattern Recognition*, vol. 4, no. 3, pp. 868 - 879, March. 2008.
- [32] J. Wiley, ed., *Digital Image Processing : Principles and Applications*, 1994.
- [33] J. G. Daugman, "High Confidence Visual Recognition of Persons by a test of Statistical Independence," *IEEE trans on pattern analysis and Machine Intelligence*, vol. 15, no. 11, pp. 1148-1160, November. 1993.
- [34] K. Zuiderveld, "Contrast Limited Adaptive Histogram Equalization," in *Graphics gems IV*, ed. P. Heckbert, pp. 474–485, Academic Press Professional, 1994.
- [35] I. Khanfir, "Contribution à l'Identification d'Individus par l'Iris," thesis for obtaining the PhD in Electrical Engineering from the National Engineering School of Sfax, Tunisia, 2009.
- [36] K. Kpalma, "Caractérisation de Textures par l'Anisotropie de la Dimension Fractale," *Proc. 2nd African Conference on Research in Computer Science*, Paris, ORSTOM, pp. 333-347, Oct. 1994.
- [37] H. Mohabeer, K. M. S. Soyjaudah and N. Pavaday, "Enhancing The Performance Of Neural Network Classifiers Using Selected Biometric Features", *Proc. 5th International Conference on Sensor Technologies and Applications*, French Riviera, Nice/Saint Laurent du Var, France, August. 2011.
- [38] K. He, G. Meeden, "Selecting the Number of Bins in a Histogram: a Decision Theoretic Approach", *Journal of Statistical Planning and Inference*, vol. 61, no.1, May. 1997.
- [39] W. L. May and W.D. Johnson, "A SAS Macro for Constructing Simultaneous Confidence Intervals for Multinomial Proportions", *Computer Methods and Programs in Biomedecine*, vol. 53, no. 3, pp. 153–162, July. 1997.
- [40] C. P Sison and J. Glaz, "Simultaneous Confidence Intervals and Sample Size Determination for Multinomial Proportions", *Journal of the American Statistical Association*, vol. 90, no. 429, pp. 366-369, 1995.
- [41] Mira Jr. J., Neto H. V., Nevesand E. B, Schneider F. K., "Biometric-oriented Iris Identification Based on Mathematical Morphology", *Journal of Signal Processing Systems*, vol. 80, no. 2, pp. 181-195, Aug. 2015.
- [42] Saminathan, K., Chakravarthy, T., and M. Chithra Devi. "Iris Recognition Based On Kernels Of Support Vector Machine", *Ictact Journal on Soft Computing*, Volume: 05, Issue: 02, pp, 889-895, 2015.
- [43] Rathgeb C., Uhl A., Wild P., and Hofbauer H., "Design Decisions for an Iris Recognition SDK," in *Handbook of Iris Recognition*, K. W. Bowyer and M. J. Burge, Eds. Springer London, pp. 359–396, 2016.

- [44] Rai, H, Yadav. Iris recognition using combined support vector machine and Hamming distance approach. ScienceDirect, Expert Systems with Applications 41: pp. 588-593, 2014.

- [45] Abiyev, R.H., Altunkaya, K., 2008. Personal Iris Recognition Using Neural Network, International Journal of Security and its Applications Vol. 2, No. 2, April, 2008.
- [46] Ali, H., and Salami, M. Iris Recognition System Using Support Vector Machines, in Biometric Systems, Design and Applications, Edited by Mr Zahid Riaz, In Tech, 2011, pp169-182, 2008.
- [47] Maria D, Alfredo P. and Stefano R.," Iris Recognition through Machine Learning Techniques: a Survey. "Pattern Recognition Letters 82 : 106-115, 2016.